



Hydrolysis and thermolysis of urea and its decomposition byproducts biuret, cyanuric acid and melamine over anatase TiO₂

Andreas M. Bernhard, Daniel Peitz, Martin Elsener, Alexander Wokaun, Oliver Kröcher*

Paul Scherrer Institut, OVGA/112, 5232 Villigen PSI, Switzerland

ARTICLE INFO

Article history:

Received 25 August 2011

Received in revised form 7 December 2011

Accepted 9 December 2011

Available online 17 December 2011

Keywords:

Biuret hydrolysis
Melamine hydrolysis
Anatase TiO₂
Urea-SCR
HPLC

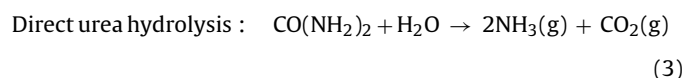
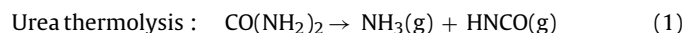
ABSTRACT

A major problem in the selective catalytic reduction of NO_x with urea (urea-SCR) is the formation of urea decomposition byproducts, which can be suppressed by the use of TiO₂ as a hydrolysis catalyst. Temperature programmed desorption and reaction (TPD/R) experiments with urea, biuret, triuret, cyanuric acid and melamine on TiO₂-coated and inert cordierite monoliths were used to investigate the reaction network of urea byproduct formation and decomposition over anatase TiO₂. All investigated compounds were found to be catalytically hydrolyzed over TiO₂. Biuret was directly hydrolyzed to urea in one step, whereas melamine hydrolyzed step-wise via ammeline and ammelide to cyanuric acid. Finally, cyanuric acid completely hydrolyzed to ammonia and carbon dioxide. The formation of byproducts was strongly favored in the absence of water. A reaction network was developed for the uncatalyzed and catalytic decomposition of urea, showing the most important reactions of urea, isocyanic acid, biuret, triuret, cyanuric acid, ammelide, ammeline and melamine under low-temperature operating conditions in SCR systems. Our results support the approach of using a special hydrolysis catalyst for urea decomposition or of catalytic coatings on exhaust pipes to avoid byproduct formation.

© 2011 Elsevier B.V. All rights reserved.

1. Introduction

Aqueous urea solution is widely used as ammonia storage compound for the selective catalytic reduction (SCR) process. Urea is inexpensive, non-toxic and decomposes according to reactions (1) and (2) to yield the actual reducing agent NH₃. According to Todorova et al., there may also be an additional reaction pathway without intermediate isocyanic acid (HNCO) formation (reaction (3)) [1].

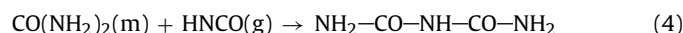


Abbreviations: cps, cells per square inch; CYA, cyanuric acid; DSC, differential scanning calorimetry; FTIR, Fourier transform infrared; GHSV, gas hourly space velocity; SCR, selective catalytic reduction of NO_x; STP, standard pressure and temperature for gases ($T=0^\circ\text{C}$, $p=1013.25\text{ hPa}$); TGA, thermogravimetric analysis; TPD/R, temperature programmed desorption and reaction.

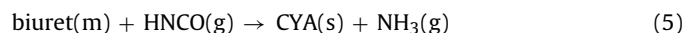
* Corresponding author. Tel.: +41 56 310 20 66, fax: +41 0 56 310 21 99.

E-mail addresses: andreas.bernhard@psi.ch (A.M. Bernhard), daniel.peitz@psi.ch (D. Peitz), martin.elsener@psi.ch (M. Elsener), alexander.wokaun@psi.ch (A. Wokaun), oliver.kroecher@psi.ch (O. Kröcher).

Unfortunately, the use of urea solution is associated with disadvantages including possible formation of solid deposits consisting of condensed urea and decomposition byproducts. The formation of byproducts is basically a consequence of the highly reactive intermediate HNCO participating in reactions other than hydrolysis [2,3]. Starting above the melting point of urea at 133°C [4], biuret is formed in the reaction of HNCO with urea (reaction (4)) [5].



The often observed byproduct cyanuric acid (CYA) is mainly formed between 190 and 250°C according to Eq. (5) [5,6].



Further possible byproducts, which are sometimes observed in minor quantities, include the triazines ammelide, ammeline, melamine and the heptazines melam and melem [2,7–9].

In general, the formation of byproducts is reversible. Different thermal and catalyzed decomposition reactions of the byproducts are reported in the literature. For instance, biuret decomposes again into urea and HNCO above 193°C [6]. CYA was found to be stable up to a temperature of 250°C , where sublimation starts, but significant thermal decomposition into HNCO was only observed between 320 and 330°C [6]. Depolymerization of CYA over Al₂O₃ in the absence of water is known as a convenient method to generate HNCO in the

laboratory [10,11]. Zahn et al. reported the catalyzed hydrolysis of CYA, melamine and derivatives over Al_2O_3 [12]. Mixing of urea with SCR catalyst powder was reported to improve the decomposition of urea and also the decomposition of byproducts [2,13]. In most of the studies on urea and byproduct formation and decomposition, TGA and DSC were applied and the starting material was administered in a crucible [2,5,6,13], which induced a slow mass transport from the starting material to the gas phase. In reality, mass transport is much faster, as urea solution is nebulized to fine droplets when injected into the exhaust gas. When these droplets hit the walls of the exhaust pipe or the catalyst, they may rebound to the gas phase, splatter to smaller droplets or form a thin film [14–16]. In any of these cases, urea evaporation and decomposition to the gas phase should be easier than in experiments using solid urea in a crucible. In our study, monoliths were impregnated with a thin layer of the starting materials as described in [17,18], in order to better represent the actual conditions in the exhaust pipe than in the previous TGA studies.

2. Experimental

2.1. Setup, analytics and measuring procedure

Experiments were carried out using a tubular quartz reactor with an inner diameter of 28 mm. Inert or catalyst-coated cordierite monoliths were impregnated with urea, biuret, melamine or CYA. The experimental parameters were as follows, unless indicated differently: Model gas: 10% O_2 , 5% H_2O in N_2 , gas flow rate = 431 L/h at STP, GHSV = 100,000 h^{-1} . Water was provided by a saturator. For the dry experiments, the water saturator was bypassed and traces of water were removed by a P_4O_{10} cartridge. More details on the setup can be found in [17].

The monoliths were impregnated by dipping into aqueous solutions. For biuret and CYA, which show limited solubility in water, the solutions had to be heated. Melamine was suspended in water at room temperature. TiO_2 -coated cordierite sheets were impregnated with urea, CYA and melamine likewise and investigated by optical microscopy. CYA and melamine were found to be present as small particles on the TiO_2 surface. CYA crystals must have grown in the supersaturated solution due to cooling and evaporation of the solvent. In the case of urea, no particles were visible. Assuming that urea was present as a smooth film, impregnation with 50 mg urea resulted in a film thickness of about 3 μm (geometric monolith surface $\approx 120\text{ cm}^2$). The amount of urea, biuret or CYA coated on the monoliths was measured by weighing the wet monoliths and multiplying the weight of the solution by its concentration. Alternatively, the amount of starting material was calculated after the experiments, based on the carbon balance or the reaction equations, which explain the formation of the observed product compounds (see Section 3.2). For biuret and CYA, the calculated amount of starting material may be more accurate than the value obtained by weighing, since evaporation of the hot solution from the monolith led to underestimation of the wet weight. For melamine, only the calculated value was available, because the effective concentration of the suspension was not known. The conversion was always based on the calculated amount of starting material. Urea was obtained from Merck at $\geq 99.5\%$ purity (p.a.); biuret, CYA and melamine were obtained from Fluka at $>98\%$ purity.

Gaseous product compounds with low molecular weight were measured by FTIR spectroscopy using a multi-component analysis method developed in-house [19]. Condensable high molecular weight compounds, which tend to form aerosols, were analyzed by a liquid-quench of the product gas, followed by HPLC analysis as described in [8,17]. The absorbing solution was the HPLC eluent

itself: 5 mM phosphate buffer, set to pH 10.4 by NaOH. In this solution, reactive HNCO is stabilized in the form of NaOCN, while urea decomposition is avoided by the fast temperature drop. Liquid samples were collected at intervals of 2.5–6 min. The sampling intervals correspond to the concentration steps plotted in Figs. 6 and 7. In addition to temperature programmed desorption and reaction (TPD/R) experiments at a temperature ramp of 10 K/min, experiments at constant temperature were carried out. The reactor was heated to a selected temperature, kept at this temperature for a certain time and then the reaction was quenched by pulling the monolith out of the hot reactor and letting it cool down under ambient conditions. The solid compounds on the monolith were washed off and analyzed by HPLC. In detail, the monoliths were first washed in the HPLC eluent overnight at RT and then boiled in pure water for a few minutes. One monolith that had been used for melamine hydrolysis, was boiled in water for 5 min (without prior washing in the eluent) and then exposed in the reactor for a TPD, according to which the washing efficiency was 90% (based on nitrogen). The stability of the byproducts in the eluent was checked by boiling an HPLC standard solution containing 10 ppm of biuret, triuret, melamine, ammeline, ammelide and 100 ppm of CYA for 15 min. The boiling decreased the triuret concentration significantly, but the other compounds appeared to be stable. Since the predominant share of the reactants and products were washed off from the monolith with eluent already at RT, further decomposition could be neglected. In some isothermal experiments, three liquid-quench samples were taken sequentially while the temperature was stable.

2.2. Catalyst coating and characterization

Cordierite monoliths with a cell density of 400 cpsi (≈ 62 cells per cm^2) and dimensions of 20 mm length, 17.5 mm width, 12.4 mm height and 117 channels were coated with anatase TiO_2 powder (DT-51 from Crystal Global). The TiO_2 powder was suspended in a diluted aqueous ammonia solution. With this procedure, active masses of about 0.6 g were realized on the monoliths. The stability of the coating was improved using a colloidal silica binder (Ludox AS-40, 10% of the catalyst mass). The monoliths were calcined at 550 $^\circ\text{C}$ for 5 h. The activity of the silica binder could be neglected, because a silica catalyst with a high surface area of 380 m^2/g showed only low urea conversion. Moreover, in a previous study on HNCO hydrolysis, silica demonstrated to be not very active for this reaction as well [20].

The specific surface area of the anatase TiO_2 catalyst coating was 89 m^2/g , measured by nitrogen physisorption on a Quantachrome Autosorb 1-c instrument. The surface was calculated using the BET method, considering adsorption data points with relative pressures (p/p_0) of 0.05–0.3 in steps of 0.05. The average pore diameter was 18 nm (mesopores) and the total pore volume was 0.41 cm^3/g at $p/p_0 = 0.993$. The sample for the physisorption measurement was prepared by calcining dried catalyst suspensions under the same conditions as the coated monoliths. Also, the specific surface area of a crushed inert cordierite monolith was measured, which yielded an insignificantly low value. The crystallinity of the untreated catalyst powder was checked by X-ray diffraction (XRD). The diffraction pattern showed excellent agreement with the theoretical diffraction pattern of anatase TiO_2 . The particle size of the untreated catalyst powder was $\text{D}_{50} = 1.70\text{ }\mu\text{m}$, measured on a Horiba LA-950 laser diffraction particle analyzer. The thickness of the coating was estimated based on data given in [10], according to which the density of the TiO_2 wash coat is 0.23 g/cm^3 . The resulting thickness for our coating is 0.2 mm.

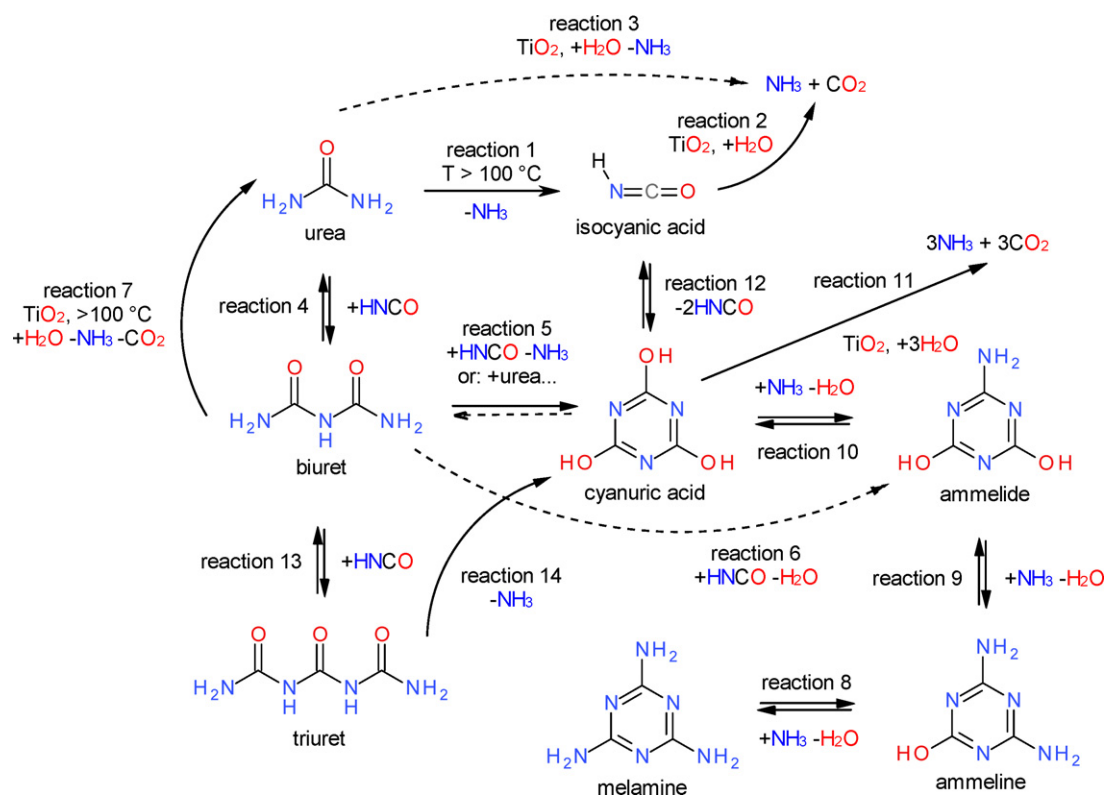


Fig. 1. Reaction network for urea decomposition with byproduct formation and decomposition.

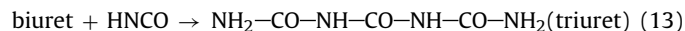
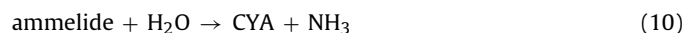
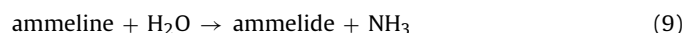
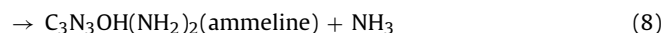
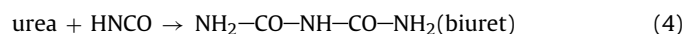
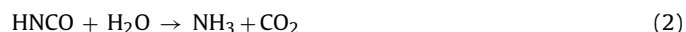
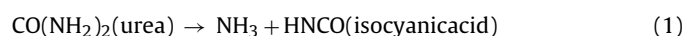
3. Results and discussion

3.1. Overview

A summary of the observed urea decomposition reactions, including byproduct formation and decomposition, is shown in Fig. 1 and will be used as a reference point in the discussion of the resulting reaction network.

Unlike analogous schemes reported in the literature [2,6], our scheme was not derived from TGA/DSC experiments with samples placed in a crucible, but from flow reactor experiments with impregnated monoliths, which should better simulate the conditions in actual urea-SCR applications. Moreover, the main focus of our study was reactions occurring over anatase TiO_2 as a hydrolysis or thermolysis catalyst. Based on these experiments, we were able to significantly clarify urea decomposition chemistry.

In the following list of equations, all the reactions shown in Fig. 1 are listed:



3.2. Biuret decomposition

Fig. 2 shows the hydrolysis of urea (a) and biuret (b) over TiO_2 . In accordance with the literature, urea was completely hydrolyzed over the catalyst and no byproduct formation was detected (Fig. 2a) [3,10,19,21]. Urea decomposition is not further discussed in this article, as it will be the subject of another article, including results from ongoing experiments. Biuret was completely hydrolyzed as well (Fig. 2b), which suggests that this reaction was also catalyzed. In order to facilitate comparing the emissions from urea and biuret, the CO_2 -emission curve for urea hydrolysis was added to Fig. 2b. Comparison of the CO_2 -emission curves reveals that biuret hydrolysis started at a lower temperature than urea hydrolysis. Since biuret is more stable to thermal decomposition than urea [6], the low temperature offset of biuret hydrolysis indicates catalyzed biuret hydrolysis. Another feature of the experiment with biuret was a broader shape of the NH_3 and CO_2 emission curves, which is attributed to slower mass transport of biuret to the catalytically active centers. CYA production from biuret cannot explain the

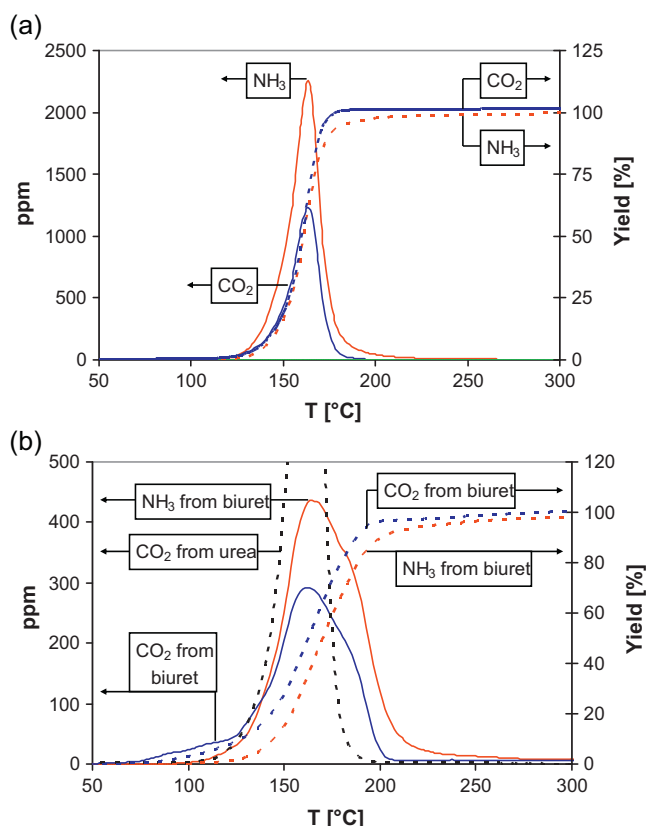


Fig. 2. Hydrolysis of urea (a) and biuret (b) over TiO_2 . Two TiO_2 -coated monoliths were placed in the reactor; the first monolith was additionally impregnated with urea or biuret; the second TiO_2 -coated monolith was clean. Parameters: Heating rate = 10 K/min, model gas: 10% O_2 , 5% H_2O in N_2 , gas flow = 431 L/h at STP, $\text{GHSV}_{\text{cat}} = 98,000 \text{ h}^{-1}$ per monolith, active masses $\approx 0.6 \text{ g}$ per monolith, $m(\text{biuret}) = 25 \text{ mg}$, $m(\text{urea}) = 48 \text{ mg}$.

broadier curves, because hydrolysis of pure CYA showed an NH_3 emission peak at 240 $^{\circ}\text{C}$ (Fig. 7c).

CO_2 emission from biuret over TiO_2 at low temperature (Fig. 2) indicates catalyzed biuret decomposition, but does not indicate whether HNCO is eliminated and then hydrolyzed (reaction (4') plus reaction (2)) or if biuret is directly hydrolyzed (reaction (7)). Hence, biuret thermolysis according to reaction (4'), without subsequent HNCO hydrolysis, was investigated under dry model gas conditions. An impregnated, TiO_2 -coated monolith was placed in the reactor. The reactor was first heated to 130 $^{\circ}\text{C}$ and then to 150 $^{\circ}\text{C}$, as shown in Fig. 3a. In spite of the dry model gas, CO_2 was still formed, which can only be explained by hydrolysis reactions with residual water in the system. Most likely, this water was adsorbed on the catalyst surface because the monolith had been impregnated with an aqueous biuret solution. Heating the reactor to 130 $^{\circ}\text{C}$ induced a prominent CO_2 peak, but the CO_2 emission dropped to a very low level within roughly 10 min (Fig. 3a). When the reactor was heated to 150 $^{\circ}\text{C}$, only little water was left on the catalyst. Fig. 3b shows the averaged quasi-stationary emission from the impregnated catalyst at 130 $^{\circ}\text{C}$ and 150 $^{\circ}\text{C}$. The time ranges considered for averaging the gaseous emissions were 26.5–42.5 min at 130 $^{\circ}\text{C}$ and 52.5–61.5 min at 150 $^{\circ}\text{C}$. For the purpose of comparison, emissions from an impregnated, inert monolith and from a urea thermolysis experiment are included in Fig. 3b. After heating to 150 $^{\circ}\text{C}$, the biuret thermolysis reaction was quenched, the monolith was washed and the washing solution was analyzed by HPLC (Table 1).

The comparison shown in Fig. 3b reveals that biuret was quite stable in the absence of the catalyst (columns 1, 4 and 6). Even at

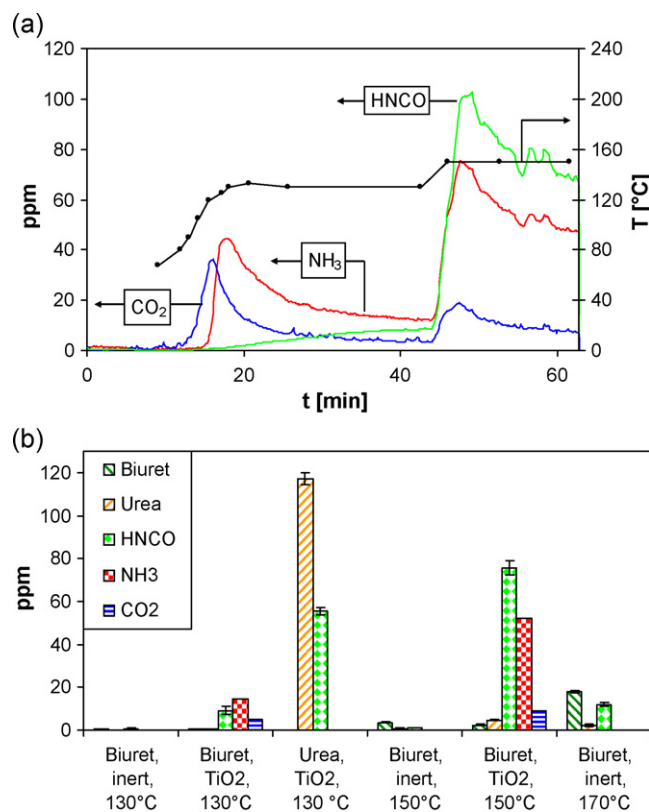


Fig. 3. Dry biuret and urea thermolysis over TiO_2 . One impregnated, TiO_2 -coated monolith was placed in the reactor. a) Gaseous emissions from biuret thermolysis during heat up at 130 $^{\circ}\text{C}$ and 150 $^{\circ}\text{C}$ measured by FTIR spectroscopy. b) Non-catalyzed biuret thermolysis at 130 $^{\circ}\text{C}$, 150 $^{\circ}\text{C}$ and 170 $^{\circ}\text{C}$ (columns 1, 4 and 6) compared to catalyzed biuret thermolysis (columns 2 and 5) and catalyzed urea thermolysis (column 3). For the catalyzed urea thermolysis, urea was desorbed from an inert monolith and then passed through a clean, TiO_2 -coated monolith. Parameters: Model gas: 10% O_2 in N_2 (dry), gas flow = 431 L/h at STP, $\text{GHSV}_{\text{cat}} = 98,000 \text{ h}^{-1}$, active mass $\approx 0.6 \text{ g}$, $m(\text{biuret on catalyst}) = 130 \text{ mg}$ (calc. from carbon balance) or 84 mg (weight), conversion = 36%, $m(\text{biuret on inert monolith}) = 78 \text{ mg}$ (weight).

170 $^{\circ}\text{C}$, the main compound detected in the gas phase was unreacted biuret (rightmost column). In the presence of the catalyst, the HNCO emission dramatically increased (columns 2 and 5), indicating catalyzed biuret thermolysis (reaction (4')). Catalyzed biuret thermolysis followed by HNCO hydrolysis (reaction (4') plus reaction (2)) cannot explain the low temperature CO_2 emission from biuret shown in Fig. 2b, because urea thermolysis (reaction (1), column 3 in Fig. 3b) over TiO_2 is even faster than biuret thermolysis (reaction (4'), column 2). Hence, the low temperature CO_2 emission shown in Fig. 2b must be due to catalyzed, direct biuret hydrolysis over TiO_2 according to reaction (7).

Table 1 shows the selectivity of the biuret thermolysis reaction based on the analysis of catalyst washing solution and the gaseous emissions integrated over the complete duration of the experiment shown in Fig. 3a.

To estimate the importance of the different reactions shown in Fig. 1, we considered a set of reactions that are able to explain the formation of the observed compounds. Hydrolysis reactions were neglected, because hydrolysis was mainly caused by residual water adsorbed on the catalyst. Also, we assumed that CYA was produced by reaction of biuret with HNCO (reaction (5a)). CYA production may also proceed via ring closure of triuret (reaction (14)), but since reaction (5a) is the sum of triuret formation (reaction (13)) plus reaction (14), the experiment does not allow to distinguish between the two pathways. Hence, reactions (4'), (1), (5a), (13), (10') and (9') were considered. From the stoichiometries of the reactions and all

Table 1Detailed results on the catalyzed biuret thermolysis experiment at $T \leq 150^\circ\text{C}$ shown in Fig. 3a.

Compound	Amount (μmol)	Yield (mmol/mol-biuret)	Selectivity (mmol/mol-biuret)	Selectivity (C-%)	Selectivity (N-%)
Starting material	1290	–	–		
Unreacted biuret (s + g)	820	640	–		
NH ₃	510	400	1100	0	36
CO ₂	160	130	340	17	0
HNCO (s + g)	500	390	1100	53	35
CYA	43	33	91	14	9.1
Urea (s + g)	68	52	140	7.2	9.6
Triuret	17	13	36	5.5	4.8
Ammelide	8.9	6.9	19	2.8	2.5
Ammeline	2.6	2.0	5.4	0.8	0.9
Sum				100	98

the measured reaction products, except NH₃ and CO₂, the contributions of the considered reactions were calculated (Fig. 4). Biuret thermolysis (reaction (4')) appeared to be the predominant reaction. Reaction (4') produces equimolar amounts of urea and HNCO. HNCO was observed during the experiment with high yield, but the urea yield was much lower, because most of the produced urea was further thermolyzed (reaction (1)). The small yield of urea is in agreement with the low stability of urea against thermolysis at 130°C concluded from Fig. 3b.

To increase the yield of urea, biuret decomposition experiments were performed at only 100°C . An impregnated, TiO₂-coated monolith was placed in the reactor. The reactor was heated to 100°C and the temperature was kept constant for about 2 h. Then, the reaction was quenched and the solid compounds were washed off the monolith and measured by HPLC. For comparison, a similar experiment was performed under dry model gas conditions. Before starting the water-free experiment, the impregnated monolith was dried inside the reactor at 70°C for 1 h. Table 2 shows the yields measured by HPLC. The selectivities and the relative yields were calculated according to Fig. 5. The amounts of gaseous compounds measured by FTIR spectroscopy could not be evaluated because the concentrations were too low.

The main solid reaction product was urea. The high selectivity for urea formation is in agreement with the apparently lower activation energy for the hydrolysis of biuret to urea (reaction (7)) compared to urea hydrolysis as indicated in Fig. 2. On the other hand, if urea hydrolyzed faster than biuret, most of the produced urea would have been hydrolyzed. Under dry model gas conditions, water was still sufficiently abundant on the catalyst surface to allow for significant biuret hydrolysis. Of course, it had to be expected that drying the catalyst at 70°C would remove only part of the adsorbed water. Piazzesi et al. found, by DRIFT experiments, that some

residual OH groups are present on TiO₂ even when treated at 450°C [21]. However, in the experiment with dry model gas, the biuret conversion and the selectivity towards urea were lower, whereas the byproduct yields were higher.

Fig. 5 shows the proportions of a set of considered reactions to explain the solid products reported in Table 2. Fig. 4 was calculated likewise. As concluded from Figs. 2b and 3b, direct biuret hydrolysis was assumed (reaction (7)). Urea thermolysis (reaction (1)) was considered as the source of HNCO, which is required to explain the byproduct formation, because urea thermolysis was found to be much faster than biuret thermolysis (reaction (4')) (Fig. 3b). Biuret thermolysis (reaction (4')) was neglected because of the low temperature applied (100°C). Also, we assumed that, in spite of the presence of water, most of the intermediately produced HNCO formed CYA and triuret (reactions (5a) and (13)) instead of being hydrolyzed (reaction (2)). Further, the HNCO yield was set to zero.

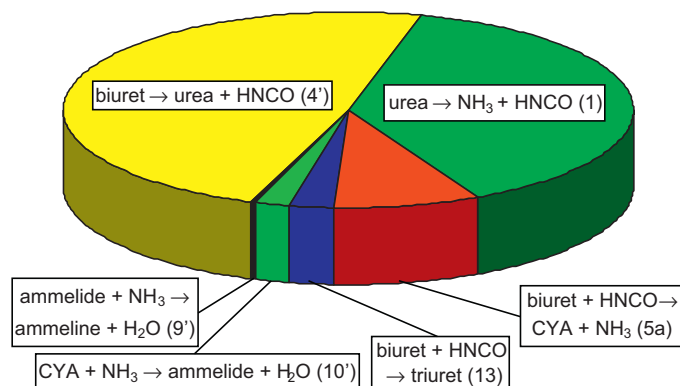
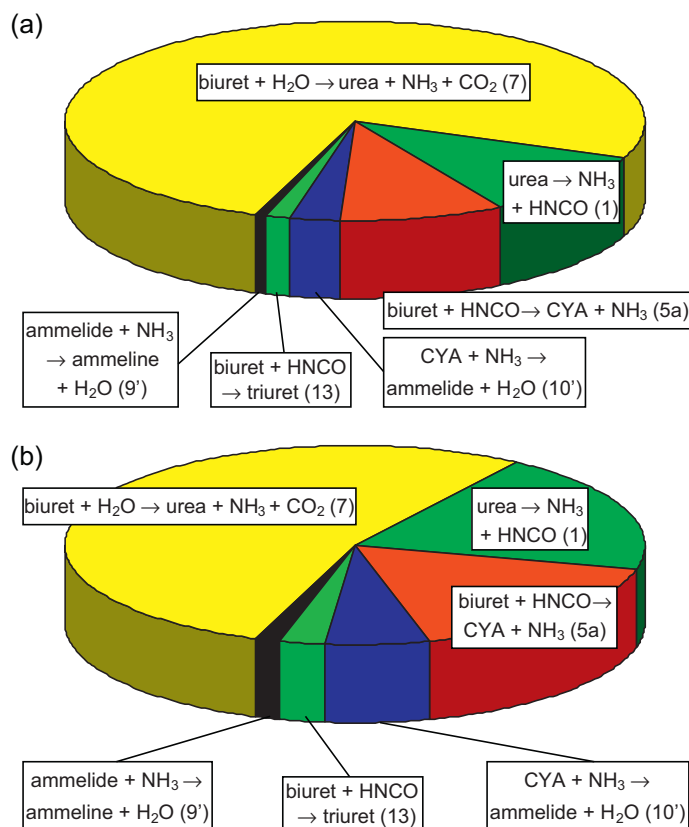
**Fig. 4.** Calculated proportions of the different reactions observed during the biuret thermolysis experiment presented in Fig. 3.**Fig. 5.** Calculated proportions of the different reactions observed during the biuret decomposition experiments presented in Table 2. a) 5% water in the model gas. b) Without water in the model gas.

Table 2

Yields and selectivities in the biuret decomposition experiments. a) Yields and selectivities. b) Selectivities in C-% and N-%. Parameters: $T = 100^\circ\text{C}$, model gas: 10% O_2 , 5% or 0% H_2O in N_2 , gas flow = 431 L/h at STP, $\text{GHSV}_{\text{cat}} = 98,000\text{ h}^{-1}$, active mass ≈ 0.6 . Experiment with 5% water: $m(\text{biuret}) = 25\text{ mg}$, conversion = 33%. Experiment with 0% water $m(\text{biuret}) = 22\text{ mg}$, conversion = 20%. The amounts of starting material and the conversions were calculated according to Fig. 5.

a)				
Compound	5% water in the model gas		0% water in the model gas	
	Yield (mmol/mol-biuret)	Selectivity (mmol/mol-biuret)	Yield (mmol/mol-biuret)	Selectivity (mmol/mol-biuret)
Urea	240	760	100	470
CYA	24	74	35	160
Ammelide	8.0	25	12	56
Triuret	4.7	15	7.6	34
Ammeline	2.5	8	4.5	20
NH_3 (calc.)	340	1100	250	1100
CO_2 (calc.)	280	880	160	730
H_2O (calc.)	−270	−840	−140	−640
b)				
Compound	5% water in the model gas		0% water in the model gas	
	Selectivity (C-%)	Selectivity (N-%)	Selectivity (C-%)	Selectivity (N-%)
Urea	23	31	23	31
CYA	23	16	23	16
Ammelide	8.4	7.5	8.4	7.5
Triuret	5.2	4.6	5.2	4.6
Ammeline	3.0	3.4	3.0	3.4
NH_3 (calc.)	0	38	0.0	38
CO_2 (calc.)	37	0	37	0.0
Sum	100	100	100	100

For the experiment with dry model gas, HNCO hydrolysis (reaction (2)) was neglected. For the experiment with wet model gas, we assumed that HNCO hydrolysis caused the decreased byproduct yield. The decrease in the absolute yields of CYA, ammelide, ammeline and triuret corresponds to a decrease in the consumption of HNCO by $9.3\text{ }\mu\text{mol}$. The proportion of reaction (2) in the experiment with water in the model gas was chosen such that $9.3\text{ }\mu\text{mol}$ HNCO were hydrolyzed. Hence, reactions (7), (1), (5a), (10'), (13), (9') and (2) were considered.

According to Fig. 5, direct biuret hydrolysis (reaction (7)) was the predominant reaction. Also, a significant amount of the urea produced seemed to have been thermolyzed (reaction (1)) to provide the HNCO required for CYA and triuret production. Still, urea remained the main solid reaction product, which supports our conclusion that the direct hydrolysis of biuret to yield urea (reaction (7)) caused the low temperature CO_2 emission shown in Fig. 2b. The following order of reaction rates was concluded from the biuret hydrolysis experiments:

Reaction (7) ($\text{biuret} + \text{H}_2\text{O} \rightarrow \text{urea} + \text{NH}_3 + \text{CO}_2$) > reaction (1) ($\text{urea} \rightarrow \text{NH}_3 + \text{HNCO}$) \approx reaction (5a) ($\text{biuret} + \text{HNCO} \rightarrow \text{CYA} + \text{NH}_3$) > reaction (2) ($\text{HNCO} + \text{H}_2\text{O} \rightarrow \text{NH}_3 + \text{CO}_2$)

3.3. Hydrolysis of melamine

It is known that melamine hydrolysis in boiling alkaline solution is a multi-step reaction yielding CYA [7]. Zhan et al. reported catalyzed melamine hydrolysis over Al_2O_3 yielding NH_3 and CO_2 [12]. The reaction proceeded apparently in one step under their experimental conditions.

Fig. 6 shows melamine sublimation from an inert monolith (a) and melamine hydrolysis over TiO_2 (b). The steps in the concentration curves are due to the intervals for collecting the liquid samples. The first sampling interval in Fig. 6a was started when the reactor reached 150°C and ended at 175°C .

When a melamine-impregnated inert monolith was heated, the melamine sublimated without detectable byproduct formation (Fig. 6a). In the presence of TiO_2 , melamine was efficiently

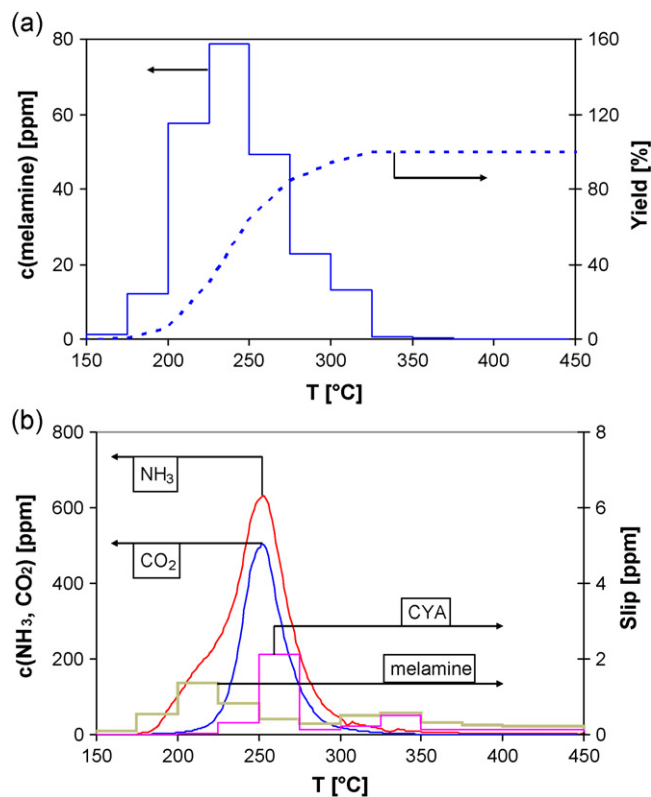


Fig. 6. a) Melamine sublimation from an impregnated inert monolith. Parameters: Model gas: 10% O_2 in N_2 (dry), $\text{GHSV}_{\text{inert}} = 97,000\text{ h}^{-1}$, $m(\text{melamine}) = 24\text{ mg}$ (calc. from carbon balance). Only HPLC analysis. b) Melamine hydrolysis over TiO_2 . Two TiO_2 -coated monoliths were placed in the reactor, the first monolith was impregnated with melamine, the second TiO_2 -coated monolith was clean. Parameters: Model gas: 10% O_2 , 5% H_2O in N_2 , $\text{GHSV}_{\text{cat}} = 98,000\text{ h}^{-1}$, active mass $\approx 0.6\text{ g}$ per catalyst-coated monolith, $m(\text{melamine}) = 22\text{ mg}$ (calc. from carbon balance). Gas flow = 431 L/h at STP.

Table 3

Summary of melamine and CYA hydrolysis TPD/R experiments (row 1: Fig. 6b, row 2: Fig. 7c, row 3: not plotted).

Row	Monolith	Starting material	Conversion (%)	NH ₃ curve features (°C)		Selectivity (mmol/mol)			
				c > 5 ppm	Peak	CO ₂	Ammeline	Ammelide	CYA
1	2 × TiO ₂	Melamine	97	178–369	253	2900	0.1	–	18
2	2 × TiO ₂	CYA	98	205–342	243	3000	–	–	–
3	Inert + 1 × TiO ₂	Melamine	68	184–338	268	2300	35	6.3	200

hydrolyzed (Fig. 6b). Interestingly, the NH₃ emission started at a lower temperature than the CO₂ emission. In all the experiments starting with a material other than melamine, the CO₂ emission started at a lower temperature than the NH₃ emission, which is attributed to the pronounced adsorption properties of NH₃. Compared to CYA hydrolysis, the NH₃ emission from melamine started 27 K below (rows 1 and 2 in Table 3).

The early NH₃ emission observed during melamine hydrolysis indicates a multi-step reaction pathway, where the amine groups were hydrolyzed first according to reactions (8)–(10) and CYA was produced as an intermediate. Only cleavage of the triazine ring (reaction (11)) at higher temperature results in CO₂ emission. In agreement with the assumption of intermediate CYA formation, a small CYA slip could be detected (Fig. 6b). If only one instead of two TiO₂-coated monoliths was used, the intermediates ammeline and ammelide were detected as well (row 3 in Table 3).

The formation of intermediates in the multi-step hydrolysis of melamine was further investigated by an isothermal experiment at 160 °C. An impregnated, TiO₂-coated monolith was heated to 160 °C for approximately 1 h. The reaction was then quenched, the monolith was washed and the washing solution was analyzed by HPLC. The melamine desorption was measured in the time interval of 28–43 min and linearly extrapolated to the whole time range for calculating the conversion. Table 4 shows the yields and selectivities of the reaction. In an analogous experiment at 165 °C, more CYA and less ammeline were formed (rightmost column).

The observed selectivities indicate the following order of reaction rates:

Reaction (8) (melamine + H₂O → ammeline + NH₃) ≈ reaction (10) (ammelide + H₂O → CYA + NH₃) > reaction (9) (ammeline + H₂O → ammelide + NH₃) > reaction (11) (CYA → 3NH₃ + 3CO₂)

3.4. Hydrolysis and de-polymerization of cyanuric acid

It is known that the hydrolysis (reaction (11)) [12] and the de-polymerization (reaction (12)) of CYA are catalyzed over Al₂O₃ [10]. Our results show that TiO₂ catalyzes these reactions as well. Fig. 7a shows CYA desorption from an inert monolith, Fig. 7b shows CYA thermolysis and Fig. 7c shows CYA hydrolysis over TiO₂.

CYA sublimed from an impregnated inert monolith (Fig. 7a) with lower vapor pressure than melamine (Fig. 6a). In addition to CYA, small amounts of biuret, HNCO, ammelide and ammeline were detected; the total yield of these byproducts was 6 mass % (5 C-%, 7 N-%). For the dry CYA depolymerization over TiO₂ shown in Fig. 7b, a clean, catalyst-coated monolith was placed downstream of a cyanuric-acid-impregnated inert monolith. Due to the catalyst, 63% of the CYA was depolymerized into HNCO. The reaction was highly selective; no byproducts could be detected. It is important to mention that NH₃ and CO₂ could not be measured, since FTIR spectroscopy was not applied in the experiments presented in Fig. 7a and b. Fig. 7c shows CYA hydrolysis over TiO₂, followed by FTIR spectroscopy. Two TiO₂-coated monoliths were placed in the reactor, the first was impregnated and the second was clean. CYA was almost completely hydrolyzed due to the catalyst. Only 1.4% of the CYA was emitted unconverted and no byproducts were detected by HPLC analysis. The shoulders in the emission curves

in Fig. 7c are attributed to a mass transport limitation from CYA grains to the active catalyst centers. Indeed, CYA grains in the size of roughly 30–200 μm were observed on the TiO₂ surface by optical microscopy.

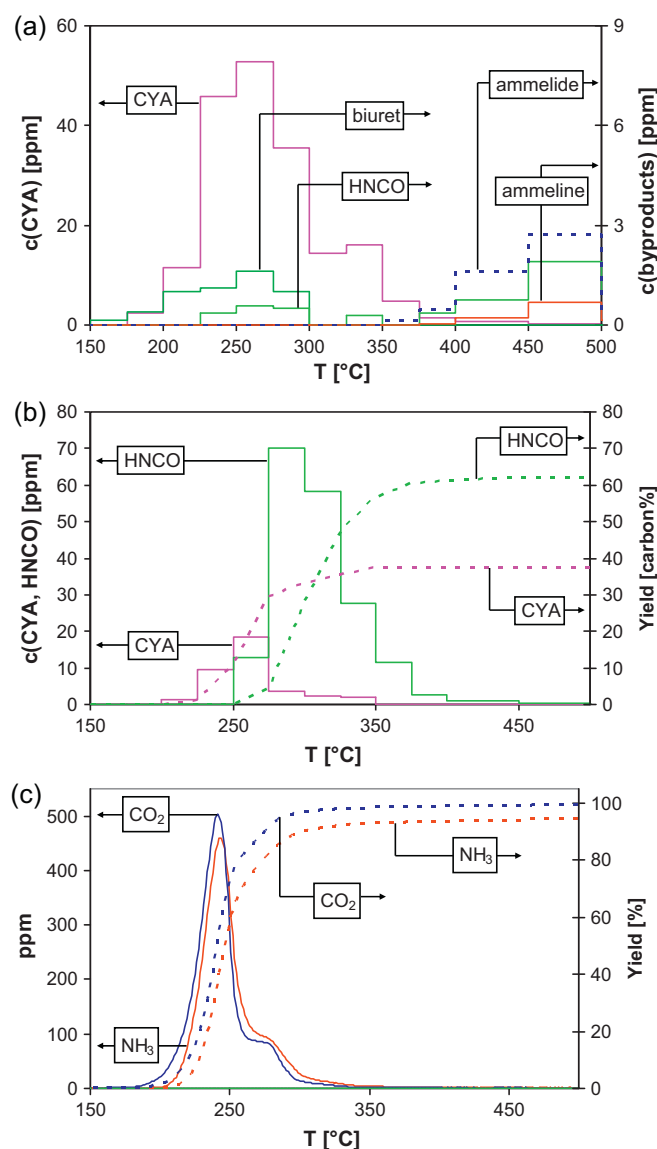


Fig. 7. a) CYA desorption from an impregnated inert monolith. Parameters: Model gas: 10% O₂ in N₂ (dry), m(CYA) = 20 mg (calc. from carbon balance). Only HPLC analysis. b) CYA thermolysis over TiO₂. CYA was desorbed from an inert monolith and then passed through a TiO₂-coated monolith. Parameters: Model gas: 10% O₂ in N₂ (dry), m(CYA) = 11 mg (calc. from carbon balance) or 10 mg (weight). Only HPLC analysis. c) CYA hydrolysis over TiO₂. Two TiO₂-coated monoliths were placed in the reactor, the first monolith was impregnated, the second monolith was clean. Parameters: Model gas: 10% O₂, 5% H₂O in N₂, m(CYA) = 23 mg (weight). Gas flow = 431 L/h at STP, GHSV_{inert} = 97,000 h⁻¹, GHSV_{cat} = 98,000 h⁻¹, active mass ≈ 0.6 g per catalyst-coated monolith.

Table 4
Melamine hydrolysis over TiO₂ at 160 °C. Parameters: Model gas: 10% O₂, 5% H₂O in N₂, gas flow=431 L/h at STP, GHSV_{cat}=98,000 h⁻¹, active mass≈0.6 g, m(melamine)=8.3 mg (calc. from carbon balance, neglecting CO₂), conversion=75.4%. Additionally, selectivities from an analogous experiment at 165 °C are shown.

Compound	Yield at 160 °C (mmol/mol-melamine)	Selectivity at 160 °C			Selectivity at 165 °C		
		(mmol/mol)	(C-%)	(N-%)	(mmol/mol)	(C-%)	(N-%)
Ammeline	400	530	53	44	130	13	11
CYA	340	450	45	22	750	75	37
Ammelide	15	20	2.0	1.3	70	6.5	4.3
Biuret	3.4	4.5	0.3	0.2	30	1.8	1.4
NH ₃	1100	1500	–	24	2500	–	42
CO ₂	Neglected	110	3.8				
HNCO			0.8	0.4			
Sum			100	92		100	96

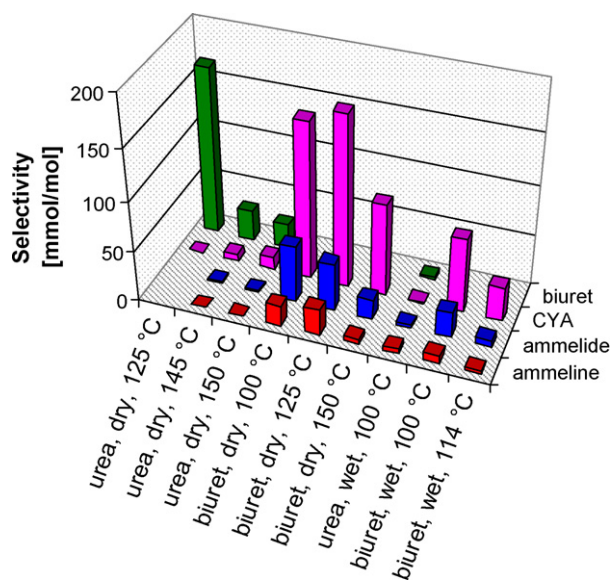


Fig. 8. Formation of solid byproducts in the experiments presented in Table 5.

3.5. Cyanuric acid formation

CYA formation could, in principle, proceed via reactions (5a)–(5c), (10), (12') and (14). The present results do not allow for definite evaluation of the contribution of each of these or to elucidate further reactions. Yet, some conclusions can be made. Table 5 and Fig. 8 summarize our results relating to CYA production from urea or biuret.

A significant amount of CYA was produced during biuret thermolysis at 125 °C (row 5 in Table 5). By contrast, from urea under similar conditions, very little CYA but significant biuret production was observed (row 1). The weak CYA production from urea indicates that HNCO preferentially reacts to form biuret (reaction (4)) rather than CYA (reaction (5a) or reaction (12)). Combination of HNCO and biuret to form ammelide (reaction (6)) does not

seem to be important, as less ammelide than CYA was formed. Since a large amount of ammonia relative to water was present on the catalyst surface, it is plausible that ammelide and ammeline were formed in reactions with ammonia (reactions (10'), (9')). The combination of biuret with urea (reaction (5b)) seems to be unimportant, as the biuret produced during urea thermolysis (row 1 in Table 5) did not react further to produce CYA.

Interestingly, CYA was also produced from biuret under wet model gas conditions at only 100 °C (row 8 in Table 5), indicating that HNCO preferentially formed CYA (reaction (5a)) instead of being hydrolyzed (reaction (2)). The stability of HNCO on the TiO₂ surface required for reaction (5a) is plausible, because Piazzesi et al. reported a steep drop of the HNCO hydrolysis activity when the temperature was decreased from 150 °C to 100 °C [21]. Also, results from ongoing experiments on urea decomposition indicate that urea thermolysis activity does not drop as steeply as the hydrolysis activity, which should allow a significant surface concentration of HNCO to be built up at low temperature. Biuret hydrolysis at 100 °C was discussed in Section 3.2. In contrast to biuret hydrolysis, urea hydrolysis at 100 °C did not yield significant amounts of byproducts (row 7 in Table 5). It is possible that a large fraction of the intermediately produced HNCO reacted with urea to form biuret as another intermediate (reaction (4)) and the biuret was then directly hydrolyzed (reaction (7)).

Alternatively, HNCO hydrolysis (reaction (2)) at 100 °C might still be too fast to allow CYA formation by reaction of biuret with HNCO (reaction (5a)). In this case, biuret dimerization (reaction (5c)) might be the reason for the CYA formation observed during biuret hydrolysis at 100 °C (row 8 in Table 5). However, the difference in the temperature dependence of CYA formation under either dry or wet model gas conditions supports the assumption that HNCO is needed for CYA formation. When the temperature for biuret decomposition under dry model gas was increased from 100 °C to 125 °C, the CYA yield remained quite constant (rows 4 and 5 in Table 5). At 150 °C, CYA formation was moderately decreased, which was most probably caused by the HNCO desorption (row 6 in Table 5). By contrast, wet model gas induced a decreased CYA formation at 100 °C, with a further decrease at 114 °C (rows 8 and

Table 5
Summarized results for CYA formation from urea and biuret. TiO₂-coated monoliths were impregnated with urea or biuret and exposed to selected temperatures.

Row	Comp.	T (°C)	Gas	Selectivities (mmol/mol)								
				CYA	Ammelide	Ammeline	HNCO	Urea	Biuret	Triuret	CO ₂	NH ₃
1	Urea	125	Dry	0.4			310		170	2.7	230	1300
2	Urea	145+	Dry	7.2	1.6	0.1	890		30	6.7	No FTIR	
3	Urea	150+	Dry	12	1.5	0.2	890		23	6.8	No FTIR	
4	Biuret	100	Dry	160	56	20	0	470		34	FTIR ignored	
5	Biuret	125	Dry	170	46	26	710	450		38	No FTIR	
6	Biuret	≤150	Dry	91	19	5.4	1100	140		36	340	1100
7	Urea	100	Wet	0.9	2.8	4.6	40		2.4	0	930	2000
8	Biuret	100	Wet	74	25	8	0	760		15	FTIR ignored	
9	Biuret	114	Wet	34	6.2	2.8	26	240		2.3	1600	2100

9 in Table 5). HNCO hydrolysis (reaction (2)) is likely to explain the decreased CYA formation by reducing the amount of HNCO available for reaction (5a). If biuret dimerization (reaction (5c)) was the main reaction pathway for CYA formation, more CYA should have been produced from biuret under wet model gas conditions. Further, the combination of biuret with urea (reaction (5b)), which is an analogous reaction, seemed to be unimportant as well (row 1 in Table 5) and simultaneous elimination of two NH_3 molecules plus one HNCO molecule seems unlikely. Hence, the following order of reaction rates at 100°C is a plausible conclusion from Table 5:

Reaction (4) (urea + HNCO \rightarrow biuret) > reaction (5a) (biuret + HNCO \rightarrow CYA + NH_3) > reaction (2) ($\text{HNCO} + \text{H}_2\text{O} \rightarrow \text{NH}_3 + \text{CO}_2$)

4. Conclusions

Thermolysis and hydrolysis of urea decomposition byproducts were investigated with and without anatase TiO_2 as a catalyst under flow reactor conditions. TiO_2 was found to catalyze the hydrolysis of all the investigated compounds including urea, biuret, melamine and CYA. It was shown that biuret is directly hydrolyzed in one step to urea, whereas melamine is hydrolyzed in a multi-step reaction. First, the amine groups are substituted to yield CYA, which is then completely hydrolyzed.

As expected, byproduct formation was favored in the absence of water. If urea was the starting material, significant amounts of biuret and only small amounts of CYA were formed, indicating that the reaction of HNCO with urea to form biuret is faster than the reaction with biuret. Using biuret as the starting material largely increased CYA formation. Interestingly, CYA was also produced during biuret hydrolysis at only 100°C , indicating that the combination of HNCO with biuret was even faster than HNCO hydrolysis at the low temperature applied.

Regarding urea-SCR, our results emphasize the suitability of anatase TiO_2 as a specialized catalyst for urea hydrolysis. Also, TiO_2 appears to be suitable for use as an anti-deposit-coating for exhaust pipes, since condensed urea, as well as the eventually formed

byproducts, will be hydrolyzed efficiently in the presence of TiO_2 . However, there may still be the need for operating intervals at elevated engine loads to increase the exhaust gas temperature above 200°C , where CYA can be hydrolyzed on the heated TiO_2 surface.

Acknowledgement

Funding by TOTAL (France) is gratefully acknowledged. TOTAL was not involved in the study design, collection, analysis or interpretation of data, nor was it involved in the preparation of the article.

References

- [1] T. Todorova, D. Peitz, O. Kröcher, A. Wokaun, B. Delley, J. Phys. Chem. C 115 (2011) 1195–1203.
- [2] M. Eichelbaum, R.J. Farrauto, M.J. Castaldi, Appl. Catal., B 97 (2010) 90–97.
- [3] A. Lundström, T. Snelling, P. Morsing, P. Gabrielsson, E. Senar, L. Olsson, Appl. Catal., B 106 (2011) 273–279.
- [4] RÖMPP Online, Thieme.
- [5] P.M. Schaber, J. Colson, S. Higgins, E. Dietz, D. Thielen, B. Anspach, J. Brauer, Am. Lab. 1 (August) (1999) 3–21.
- [6] P.A. Schaber, J. Colson, S. Higgins, D. Thielen, B. Anspach, J. Brauer, Thermochim. Acta 424 (2004) 131–142.
- [7] B. Bann, S.A. Miller, Chem. Rev. 58 (1958) 131–172.
- [8] M. Koebel, M. Elsener, J. Chromatogr. A 689 (1995) 164–169.
- [9] O. Kröcher, M. Elsener, Chem. Eng. J. 152 (2009) 167–176.
- [10] P. Hauck, A. Jentys, J.A. Lercher, Appl. Catal., B 70 (2007) 91–99.
- [11] M. Kleemann, M. Elsener, M. Koebel, A. Wokaun, Ind. Eng. Chem. Res. 39 (2000) 4120–4126.
- [12] Z. Zhan, M. Müllner, J.A. Lercher, Catal. Today 27 (1996) 167–173.
- [13] H.L. Fang, H.F.M. DaCosta, Appl. Catal., B 46 (2003) 17–34.
- [14] F. Birkhold, U. Meingast, W. Peter, O. Deutschmann, SAE 2006-01-0643 (2006).
- [15] A. Nishioka, Y. Sukegawa, K. Katogi, H. Mamada, T. Kowatari, T. Mukai, H. Yokota, SAE 2006-01-0644 (2006).
- [16] H. Ström, A. Lundström, B. Andersson, Chem. Eng. J. 150 (2009) 69–82.
- [17] A.M. Bernhard, I. Czekaj, M. Elsener, A. Wokaun, O. Kröcher, J. Phys. Chem. A 115 (2011) 2581–2589.
- [18] A. Lundström, B. Andersson, L. Olsson, Chem. Eng. J. 150 (2009) 544–550.
- [19] O. Kröcher, M. Elsener, E. Jacob, Appl. Catal., B 88 (2009) 66–82.
- [20] G. Piazzesi, The catalytic hydrolysis of isocyanic acid (HNCO) in the urea-SCR process, Ph.D. thesis No. 16693, ETH Zurich, Switzerland, 2006, http://ega.web.psi.ch/Piazzesi_PhD_thesis_ETH_Zurich_2006.pdf.
- [21] G. Piazzesi, O. Kröcher, M. Elsener, A. Wokaun, Appl. Catal., B 65 (2006) 55–61.